# Kaon electroproduction in the Regge pole model

Byung Geel Yu,[1,*] Tae Keun Choi,[2,†] and Kook Jin Kong[1,‡]

[1] *Research Institute of Basic Sciences, Korea Aerospace University, Goyang 10540, Korea*
[2] *Department of Physics, Yonsei University, Wonju 26493, Korea*

(Dated: July 7, 2023)

A Reggeized model for the exclusive kaon electroproduction $p(e,e'K^+)\Lambda(\Sigma^0)$ is presented to describe the existing data from JLab experiments. The model includes the Reggeized meson exchanges $K(495)+K_1(1270)+K^*(892)+K_2^*(1430)$ in the $t$-channel where their coupling constants are determined from the SU(3) symmetry relation to $\pi$, $\rho$, $a_2$ and axial vector mesons with the $F/D$ ratio chosen appropriate for other experiments. The Gross-Riska charge form factors to nucleon and kaon exchanges are introduced to preserve gauge invariance of the reaction. In this work longitudinal, transverse, and unpolarized cross sections $d\sigma_L$, $d\sigma_T$, and $d\sigma_U$ are analyzed with the numerical consequences of the current model compared with those of Vanderhaeghen, Guidal, Laget (VGL) and Vrancx, Ryckebusch, Nys (VRN) models.

PACS numbers: 13.60.Le, 13.60.-r, 13.60.Rj

## I. INTRODUCTION

Understanding hadrons, which are composite particles made up of quarks and gluons, poses a fundamental challenge in the field of nuclear physics. To address this topic, the ${}^1H(e,e'K+)$ reaction has drawn our attention as a useful experimental tool that offers insights into flavor degrees of freedom while involving strangeness in the simplest possible system.

The electromagnetic form factors of hadrons directly reflect their internal structure. Measuring the transition to the asymptotic, pointlike regime is crucial for experimental verification of a key prediction of quantum chromodynamics (QCD). Consequently, the investigation of pion and kaon form factors is essential for both experimental and theoretical purposes, as evident in the existing literature.

In the case of charged kaons, which are among the simplest hadronic systems containing strangeness and are available for experimental study, a single form factor (FK) determines their structure. Experimental measurements of the kaon form factor have been conducted at low-momentum transfers (Q2 ¡ 0.2 GeV2) through elastic scattering of high-energy kaons off atomic electrons. However, to explore higher values of Q2, meson electroproduction is employed. This approach has been successfully used to extract the pion electroproduction cross section and form factor up to Q2 values of 3.91 GeV2.

Understanding the relative contributions of longitudinal and transverse terms to the meson cross section, as well as their dependence on the variables -t and Q2, is of great interest in evaluating the potential for probing the transverse spatial structure of the nucleon through meson production. Recent calculations suggest that the leading-twist behavior for light mesons can be observed at Q2 values ranging from 5 to 10 GeV2. Therefore, obtaining experimental data to validate these predictions is highly valuable.

At JLAB the exclusive reaction $p(e,e'\pi^+)n$ has been studied for a wide range of photon virtualities $Q^2$ at an invariant mass of the $\pi^+n$ system around the onset of deep inelastic scattering (DIS) regime, $W \simeq 2$ GeV [**?** **?** **?** **?** **?** ]. A separation of the cross section into the transverse $\sigma_{\rm T}$, longitudinal $\sigma_{\rm L}$ and interference $\sigma_{\rm TT}$ and $\sigma_{\rm LT}$ components has been performed. The CLAS data for the polarized beam single-spin asymmetry in $p(\vec{e},e'\pi^+)n$ are also available [**?** ]. The HERMES data at DESY [**?** ] extend the kinematic region to much higher values of $W^2$ >10 GeV$^2$ toward the true DIS region $Q^2 \gg 1$ GeV$^2$ and much higher values of $-t$. The cross section for $p(e,e'\pi^+)n$ has also been measured above the resonance region at the Cambridge Electron Accelerator (CEA) [**?** ], in $p(e,e'\pi^+)n$ and $n(e,e'\pi^-)p$ at the Wilson Synchrotron Laboratory at Cornell [**?** **?** **?** ] and DESY [**?** **?** **?** **?** **?** ]. [**?** ]

## II. ELECTROPRODUCTION OF PSEUDOSCALAR MESON

$$e(\kappa)+N(p)\to e(\kappa')+Y(p')+K(q) \tag{1}$$

The $S$-matrix element for electroproduction is[1]

[1] For photoproduction the $S$-matrix element is given by

$$S=\frac{1}{(2\pi)^2}\sqrt{\frac{MM'}{4E_\gamma q_0 k_0 EE'}}i\delta^4(p+k-p'-q)\mathcal{M}_{fi}$$

* bgyu@kau.ac.kr
† tkchoi@yonsei.ac.kr
‡ wooyoung@knu.ac.kr

$$S = \frac{1}{(2\pi)^{7/2}} \frac{m_e\sqrt{MM'}}{\sqrt{2E_\gamma q_0 \kappa_0 \kappa_0' E E'}} i\delta^4(p+k-p'-q)\mathcal{M}_f \quad (2)$$

### A. kinematics

$$\frac{d^3\sigma}{dE_e' d\Omega_e' d\Omega_K} = \Gamma \frac{d\sigma}{d\Omega_K} \quad (3)$$

where the flux of the electron current is given by

$$\Gamma = \frac{\alpha}{2\pi^2} \frac{E_e'}{E_e} \frac{K_H}{Q^2} \frac{1}{1-\epsilon}, \quad (4)$$

with the equivalent photon laboratory energy $K_H = \frac{W^2-M^2}{2M}$ and electron polarization $\epsilon = 1/\left(1 + \frac{2|\vec{k}|^2}{Q^2} \tan\frac{1}{2}\theta_e\right)$ measured by the angle $\theta_e$ deviated from the reaction plane. Separating the kinematical part of electron scattering in Eq. (2) the cross section for pion production by the virtual photon

$$\gamma^*(k) + N(p) \to Y(p') + K(q) \quad (5)$$

is expressed as follows,

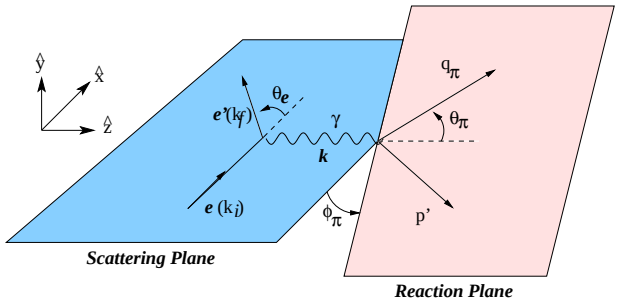


FIG. 1. Exclusive reaction $N(e,e'\pi)N'$ in the laboratory. $\phi$ stands for the azimuthal angle between the electron scattering $(e,e')$ plane and reaction $N(\gamma^*,\pi)N'$ plane.

$$\frac{d\sigma}{d\Omega_K} = \frac{d\sigma_T}{d\Omega_K} + \epsilon\frac{d\sigma_L}{d\Omega_K} + \epsilon\frac{d\sigma_{TT}}{d\Omega_K}\cos 2\Phi_K + \sqrt{2\epsilon(\epsilon+1)}\frac{d\sigma_{TL}}{d\Omega_K}\cos\Phi_K \ . \quad (6)$$

The mandelstam variables for the reaction in the three channel are

$$\begin{aligned} s &= (p+k)^2 = (p'+q)^2, \\ t &= (q-k)^2 = (p-p')^2, \\ u &= (p-q)^2 = (p'-k)^2 \end{aligned} \quad (7)$$

with the virtual photon momentum $k^2 = \kappa'^2 - \kappa^2$ in terms of the initial and the final electron momenta $\kappa$ and $\kappa'$. We denote the virtuality of photon with $Q^2 = -k^2$.

## III. THE MODEL

In this work, we utilize the effective Lagrangian approach for constructing the Born approximation amplitude to one-photon exchange at the tree level. It is, then, extended to reggeize the $t$-channel meson exchange by replacing the Feynman propagator with the Regge propagator [6**?** ].

As illustrated in Ref. [6] for kaon photoproduction, we consider an extended version of the GLV model where the tensor meson $K_2^*$ is introduced to give a better description of differential cross sections and spin polarization observables with the reduction of the large $K^*$ coupling constants of the original model to such a degree that seems to be consistent with SU(3) value.

We also discuss the recent Reggeized model by VRN to compare numerical consequences from different form factors in other models.

In this work we utilize the monopole form of the charge form factor for the exchanged mesons, $\varphi = K$, $K^*$, $K_1$, and $K_2^*$, coupling to virtual photon.

### A. Reggeized amplitude for electroproduction

For gauge invariance of the electroproduction amplitude coupling to virtual photon we use the Gross-Riska prescription [3, 9] for the charge form factors of nucleon and kaon.

In constructing the electroproduction model, we use the same physical constants as in photoproduction. Electroproduction will be an extension of these photoproduction amplitudes with charge factors introduced in the gauge invariant way. The charge form factor of kaon, $F^K(Q^2)$ which gives the leading contribution to the longitudinal cross section $\sigma_L$, can be treated as gauge invariant by including the nucleon pole in the $s$-channel with charge form factor $F_1(Q^2)$. For the gauge invariant introduction of charge form factors between kaon and nucleon, we follow the recipe by the Gross-Risk and apply to VGL model as well as the current calculation in this work. Other promising models, the VRN model includ-

ing the KM model for pion electroproduction, apply an energy-dependent cutoff masses $\Lambda_N(Q^2,s)$ to the nucleon charge form factor in order to take into account the contribution of baryon resonances in the low energy region. Moreover, since they further consider the Regge pole for the nucleon with the energy-dependent slope of kaon trajectory $\alpha'_K(t;Q^2,s)$, which is different from that of kaon pole in the $t$-channel, they adopt the approach of simply canceling with each other which is different from the GR scheme as will be discussed below.

For the hyperon $Y=\Lambda$ and $\Sigma^0$, the reggeized $K$ exchange in the $t$-channel that respects gauge invariance can be written as

$$\mathcal{M}_K = i\,\bar{u}'_Y(p')\left[eg\gamma_5\frac{(\not{p}+\not{k}+M)}{s-M^2}\widetilde{F}_1(k^2)\not{\epsilon}+e\widetilde{F}^K(k^2)\frac{(2q-k)\cdot\epsilon}{t-m_K^2}g\gamma_5\right](t-m_K^2)\mathcal{P}^K(s,t)u_N(p)\,, \tag{8}$$

where the charge coupling proton pole term is considered to preserve gauge invariance with proton and kaon charge form factors,

$$\widetilde{F}_1(k^2)\not{\epsilon}=\widetilde{F}_1'(k^2)\not{\epsilon}=F_1(k^2)\left(\not{\epsilon}-\not{k}\frac{\epsilon\cdot k}{k^2}\right)+F_1(0)\not{k}\frac{\epsilon\cdot k}{k^2}\,, \tag{9}$$

$$\widetilde{F}^K(k^2)(2q-k)\cdot\epsilon=F^K(k^2)(2q-k)\cdot\left(\epsilon-k\frac{\epsilon\cdot k}{k^2}\right)+F^K(0)(2q-k)\cdot k\frac{\epsilon\cdot k}{k^2}\,, \tag{10}$$

which are normalized by $F_1(0)=1$ and $F^K(0)=1$, respectively.

Based on Ref. [7] for photoproduction the $t$-channel meson exchange, as depicted in Fig. 2, are written as by

$$\mathcal{M}_A = i\bar{u}'(p')\frac{g_{\gamma KK_1}}{m_0}F^A(k^2)(k\cdot Q\,\epsilon_\mu-\epsilon\cdot Q\,k_\mu)(-g^{\mu\nu}+Q^\mu Q^\nu/m_A^2)\left[g^v_{ANN}\,\gamma_\nu+i\frac{g^t_{BNN}}{2M}\sigma_{\lambda\nu}Q^\lambda\right]\gamma_5\mathcal{P}^A(s,t)u(p), \tag{11}$$

$$\mathcal{M}_V = -\bar{u}'(p')\frac{g_{\gamma KK^*}}{m_0}F^{K^*}(k^2)\varepsilon^{\mu\nu\alpha\beta}\epsilon_\mu k_\nu q_\alpha(-g_{\beta\rho}+Q_\beta Q_\rho/m_V^2)\left[g^v_{VNN}\,\gamma^\rho+i\frac{g^t_{VNN}}{2M}\sigma^{\lambda\rho}Q_\lambda\right]\mathcal{P}^V(s,t)u(p)\,, \tag{12}$$

$$\mathcal{M}_T = -\bar{u}'(p')\frac{2g_{\gamma KK_2^*}}{m_0^2}\,F^T(k^2)\varepsilon^{\mu\nu\alpha\beta}\,\epsilon_\mu k_\nu q_\alpha q^\rho\Pi_{\beta\rho;\lambda\sigma}(q-k)\left[\frac{2g^{(1)}}{M}(\gamma^\lambda P^\sigma+\gamma^\sigma P^\lambda)+\frac{4g^{(2)}}{M^2}P^\lambda P^\sigma\right]\mathcal{P}^T(s,t)u(p) \tag{13}$$

with the mass parameter $m_0=1$ GeV, the $t$-channel momentum transfer $Q=q-k$, and $P=\frac{1}{2}(p+p')$.

We use $\varepsilon^{0123}=+1$.

The tensor meson spin projection is

$$\Pi^{\beta\rho;\lambda\sigma}(Q)=\frac{1}{2}(\eta^{\beta\lambda}\eta^{\rho\sigma}+\eta^{\beta\sigma}\eta^{\rho\lambda})-\frac{1}{3}\eta^{\beta\rho}\eta^{\lambda\sigma} \tag{14}$$

with $\eta^{\mu\nu}=-g^{\mu\nu}+\frac{Q^\mu Q^\nu}{m_T^2}$ .

The Regge propagator for the exchanged meson $\varphi(=K,\,K^*,\,K_1,\,K_2^*)$ is written collectively,

$$\mathcal{P}^\varphi(s,t)=\frac{\pi\alpha'_\varphi\times\text{phase}}{\Gamma(\alpha_\varphi(t)+1-J)\,\sin(\pi\alpha_\varphi(t))}\left(\frac{s}{s_0}\right)^{\alpha_\varphi(s)-J} \tag{15}$$

where the canonical form of the Regge phase is $\frac{1}{2}((-1)^J+e^{-i\pi\alpha_\varphi(t)})$ for the meson of spin-$J$.

For the valid prediction within the Regge framework, it is of significance to assign the correct phase to a Regge pole in the reaction amplitude. In consideration of the exchange-degenerate (EXD) pairs $(K,K_1)$, and $(K^*,K_2^*)$, we assume the weak EXD for $\alpha_K\approx\alpha_{K_1}$ and $\alpha_{K^*}\approx\alpha_{K_2^*}$. Hence, we choose the complex phase $e^{-i\pi\alpha_\varphi(t)}$ for all these meson exchanges, while denoting these trajectories by

$$\alpha_K(t)=0.7\,t-0.171\,, \tag{16}$$

$$\alpha_{K_1}(t)=0.7\,t-0.133\,, \tag{17}$$

$$\alpha_{K^*}(t)=0.83\,t+0.25\,, \tag{18}$$

$$\alpha_{K_2^*}(t)=0.85\,t+0.273\,. \tag{19}$$

We use the trajectories in Eqs. (16) and (18) to agree with $\gamma p\to K^{*+}(892)\Lambda$ photoproduction in Ref. [8]. The meson-baryon coupling constants between models are compared in Table I.

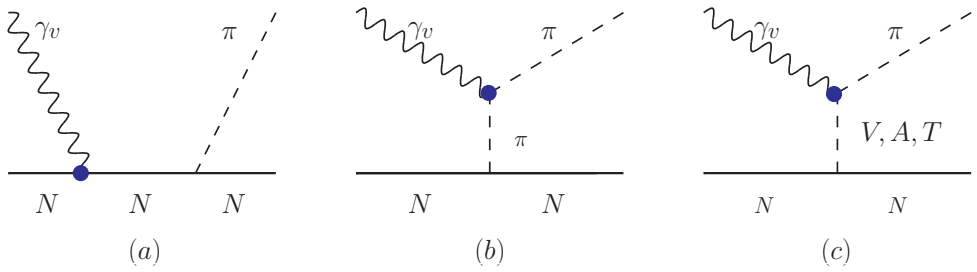


FIG. 2. The diagrams describing kaon electroproduction amplitudes in exclusive reactions $p(e, e'K^+)\Lambda$ and $p(e, e'K^+)\Sigma^0$. The nucleon pole and pion pole in (a) and (b) constitutes gauge invariant pion exchange.

### B. Charge form factors for nucleon and mesons

#### 1. *Current model and VGL model*

Given the meson exchange $K + K_1 + K^* + K_2^*$ in the current model as in Eqs. (8), (11), (12), and (13) the VGL model considers $K + K^*$ with the nucleon charge form factor in Eq. (9) as the dipole form

$$F_1(Q^2) = \frac{1 + \mu_N \tau}{1 + \tau} \left(1 + Q^2/\Lambda_N^2\right)^{-2} \tag{20}$$

and $\tau = Q^2/4M^2$. Kaon charge form factor in Eq. (10) is parameterized as a monopole of the photon momentum squared,

$$F^\varphi(Q^2) = \left(1 + Q^2/\Lambda_\varphi^2\right)^{-1}, \tag{21}$$

which will be applied to other charge form factors of mesons coupling to the virtual photon in the $t$-channel as well.

Since we have only one parameter $\Lambda_\varphi$ in each meson form factor as well as the meson-baryon coupling constants determined from $SU(3)$ flavor symmetry as shown in Table II in the Appendix, the EM structure of the hadrons can be investigated in a less model-dependent way through the form factors with the cutoff mass appropriately chosen to explain the data.

In the VGL model [1, 2] the cutoff mass for the nucleon form factor is

$$\Lambda_N = 0.843 \text{ GeV}, \tag{22}$$

and

$$\Lambda_K = \Lambda_{K^*} = \sqrt{0.6} \text{ GeV}, \text{ and } \sqrt{1.5} \text{ GeV} \tag{23}$$

are chosen, respectively, for the meson form factors in Eq. (21).

#### 2. *VRN model*

The VRN model [4] is essentially an extension of the KM model. There is no tensor meson exchange. Instead, it takes into account the vector meson $K^*(1410)$ and axial vector meson $K_1(1400)$ of other masses and uses their coupling constants from the least $\chi^2$ optimized values. Here, we select model IIb for the best $\chi^2$ fit to empirical data and compare the numerical results with the current model predictions.

In the model the trajectoryies of the $K^*$ and $K^*(1410)$ are chosen as

$$\alpha_{K^*}(t) = 0.85\, t + 0.324\,, \tag{24}$$
$$\alpha_{K^*(1410)}(t) = 0.83\, t - 0.66 \tag{25}$$

with the complex phase for the $K$ and $K^*$, but the constant phase for the latter, respectively.

- Kaon charge form factor

Charge form factors for these meson exchange are the same as given in Eq. (21) with the cutoff massese

$$\Lambda_K = \Lambda_{K^*} = \Lambda_{K^*_{1410}} = 0.838 \,\text{GeV}\,. \tag{26}$$

- Nucleon charge form factor

In the low energy region of $\pi$ electroproduction, Kaskulov and Mosel consider a recipe to include the resonance effect via a modification of the nucleon charge form factor, and it has the energy-squared $s$-dependence by introducing the $s$-dependent cutoff mass, as a result [5]. The VRN model employs the nucleon charge form factor

$$F_1(Q^2, s) = \left(1 + Q^2/\Lambda_N^2(s)\right)^{-2} \tag{27}$$

and, similar to Ref. [5], the cutoff mass is parameterized to have the $s$-dependence in the $s$-channel as

$$\Lambda_N(s) = 0.84\,\text{GeV} + 1.354 \left(1 - \frac{M_p^2}{s}\right) \text{GeV} \tag{28}$$

with the factor 1.354 GeV resulting from the difference between the cutoff masses, $\Lambda_\infty - \Lambda_N$.

In addition, given the nucleon charge form factor in Eq. (27), the slope of the $K$ trajectory in Eq. (16) is designed as the function of $Q^2$ and $s$,

$$\alpha'_K(Q^2, s) = \left(\frac{0.7}{1 + \xi \frac{Q^2}{s}}\right) \text{ GeV}^{-2} \tag{29}$$

with the constant $\xi = 2.43$ in the denominator fitted to empirical data. Thus, the kaon Regge pole has an explicit $Q^2$-dependence, $\mathcal{P}^K(s,t,Q^2)$ with the slope given by Eq. (29) for the $\alpha_K$ trajectory in Eq. (16). The nucleon pole term multiplied by the kaon Regge pole in Eq. (8) is changed to

$$F_1(Q^2)\mathcal{P}^K(s,t) \to F_1(Q^2)\mathcal{P}^K(s,t,Q^2), \qquad (30)$$

whereas the kaon pole term with the Regge propagator is given as usual

$$F_K(Q^2)\mathcal{P}^K(s,t). \qquad (31)$$

The effect of the $N^*$ contribution via a modification of the nucleon charge form factor is a feature of the KM and VRN models. Nevertheless, as can be seen in Eqs. (9) and (10), the Gross-Riska gauge prescription is not suited for such an approach because of inequality of the kaon Regge propagator between the nucleon and kaon pole terms as in Eqs. (30) and (31). The nucleon and kaon pole terms in the VRN amplitude are given independently with each form factor in Eqs. (21) and (27) and the Regge propagator as discussed in Eqs. (30) and (31). Thus, gauge invariance of the kaon exchange together with nucleon pole is restored by the gauge fixing term,

$$\mathcal{M}_{\rm GF} = eg\bar{u}(p')\gamma_5 u(p)\frac{\epsilon\cdot k}{k^2}(t-m^2)$$
$$\times\left[F^K(Q^2)\mathcal{P}^K(s,t) - F_1(Q^2,s)\mathcal{P}^K(s,t,Q^2)\right], \quad (32)$$

instead of introducing the Gross-Riska form factors $\widetilde{F}_1$ and $\widetilde{F}^K$ in the above amplitudes. In practice, no difference is in the gauge prescription between the Gross-riska and the subtraction form in Eq. (32).

### C. Meson-baryon coupling constants

We determine the meson-baryon coupling constants and the radiative decay constant from empirical informations in accordance with symmetry arguments. We use $f_\rho = 5.35 \pm 1.15$ from the $\rho$ decay, $\Gamma(\rho \to e^+e^-) = 7.04 \pm 0.06$ keV. Therefore, $g_\rho = 2.6$ for the vector coupling and $\kappa_\rho = 6.1$ for the tensor coupling of the vector meson are taken in the present work. Theoretical estimates for the radiative decay width of axial meson of type-$A$ ($^3P_1$) and -$B$ ($^1P_1$) were reported to be $\Gamma(A \to) =$ in the covariant quark model (COQM) [**?** ] and coupled channel approach [**?** **?** ].

- Radiative decay constants

$$\Gamma_{V(A)\to K\gamma} = \frac{1}{96\pi}\frac{g^2}{m_0^2}\left(\frac{m_{V(A)}^2 - m_K^2}{m_{V(A)}}\right)^3 \qquad (33)$$

$$\Gamma_{T\to K\gamma} = \frac{1}{10\pi}\frac{g^2}{m_0^4}\left(\frac{m_T^2 - m_K^2}{2m_T}\right)^5 \qquad (34)$$

TABLE I. Meson-baryon coupling constants and cutoff masses in electroproduction $\gamma^* p \to K^+\Lambda(\Sigma^0)$ [6]. Energy-dependent cutoff $\Lambda_N(s)$ is given by Eq. (28). $^{(*)}$This value is chosen as a temporary convenience to follow the similar denotation for listing coupling constants. Its product with $g^v_{K^*(1410)N\Lambda}$ yields $eG_{\gamma K^*(1410)K}G_{K^*(1410)\Lambda p}$ in Ref. [4].

| | NSC97a | VGL [2] | VRN [4] | This work |
|---|---|---|---|---|
| $g_{KN\Lambda}$ | $\lvert 13.24\rvert$ | $-11.54$ | $-13.2$ | $-11.54$ |
| $g_{KN\Sigma^0}$ | | 4.47 | | 4.47 |
| $\Lambda_K$ | | $\sqrt{1.5}$ | 0.838 | 1.2 |
| $\Lambda_N$ | | 0.843 | $\Lambda_N(s)$ | 1.55 |
| $g_{\gamma KK^*}$ | | 0.254 | 0.254 | 0.254 |
| $g^v_{K^*N\Lambda}$ | $-4.26$ | $-23$ | $-8.14$ | $-4.5$ |
| $g^t_{K^*N\Lambda}$ | $-11.31$ | $-57.5$ | $-8.47$ | $-16.7$ |
| $g^v_{K^*N\Sigma^0}$ | - | $-25$ | - | $-2.6$ |
| $g^t_{K^*N\Sigma^0}$ | - | 25 | - | 3.2 |
| $\Lambda_{K^*}$ | | $\sqrt{1.5}$ | 0.838 | 1.2 |
| $g_{\gamma KK_2^*}$ | | - | - | 0.276 |
| $g^{(1)}_{K_2^*N\Lambda}$ | | - | - | $-4.45$ |
| $g^{(2)}_{K_2^*N\Lambda}$ | | - | - | 0 |
| $g^{(1)}_{K_2^*N\Sigma^0}$ | | - | - | $-4.9$ |
| $g^{(2)}_{K_2^*N\Sigma^0}$ | | - | - | 0 |
| $\Lambda_{K_2^*}$ | | - | - | 1.5 |
| $g_{\gamma KK_1(1270)}$ | | - | - | 0.071 |
| $g^v_{K_1N\Lambda}$ | | - | - | $-6.7$ |
| $g^t_{K_1N\Lambda}$ | | - | - | 15.36 |
| $g^v_{K_1N\Sigma^0}$ | | - | - | 1.81 |
| $g^t_{K_1N\Sigma^0}$ | | - | - | $-1.4$ |
| $\Lambda_{K_1}$ | | - | - | 1.5 |
| $g_{\gamma KK^*(1410)}$ | | - | $0.2^{(*)}$ | - |
| $g^v_{K^*(1410)N\Lambda}$ | | - | 49.52 | - |
| $g^t_{K^*(1410)N\Lambda}$ | | - | 34.66 | - |
| $\Lambda_{K^*(1410)}$ | | - | 0.838 | 1.5 |

## IV. DATA ANALYSIS

### A. Differential cross sections

From the phenomenological analysis based on the model calculation, it could be made the following two tentative points.

- Dominance of kaon exchange in the longitudinal cross section $d\sigma_L$; solely determined by the single parameter $\Lambda_K$ and not sensitive to a change in other cutoff masses. Further, it is not likely that the longitudinal (or scalar) component of baryon resonances is to be significant, though contributing. Therefore, similar to pion, the case of kaon allows for a precise extraction of kaon charge form factor $F^K(Q^2)$ from the $d\sigma_L$.

- The transverse cross section $d\sigma_T$ is largely determined by the parameter $\Lambda_N$ of the nucleon Dirac form factor $F_1(Q^2)$ in comparison to other meson exchanges.

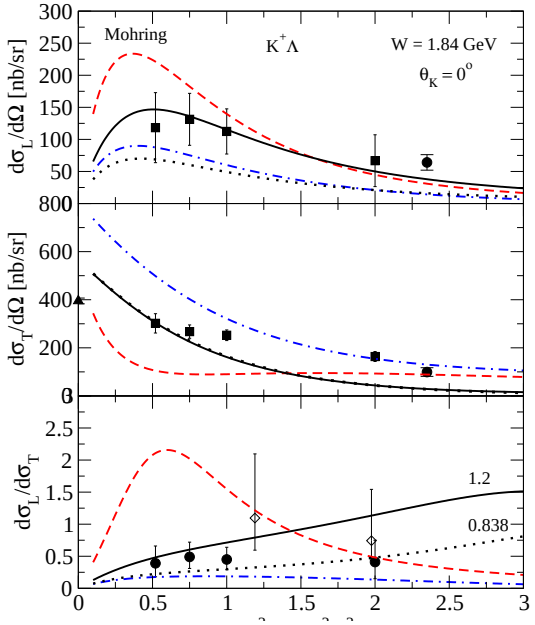


FIG. 3. $Q^2$ dependence of $d\sigma_L$, $d\sigma_T$ and the ratio $d\sigma_L/d\sigma_T$ for $K^+\Lambda$ electroproduction. Solid curves are from the current model calculation by choosing $\Lambda_K = 1.2$ GeV together with the dotted one by $\Lambda_K = 0.84$ GeV. The (red) dashed curves are from the VGL model and (blue) dashe-dotted from the VRN model predictions, respectively. In what follows we keep these notations for the curve. Data are taken from Ref. [10**?** ]

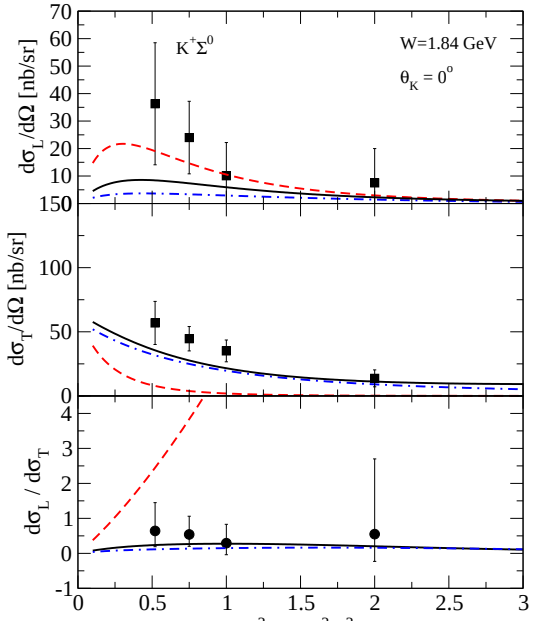


FIG. 4. $Q^2$ dependence of $d\sigma_L$, $d\sigma_T$ and the ratio $d\sigma_L/d\sigma_T$ for $K^+\Sigma^0$ electroproduction. Data are taken from Ref. [10]

It is crucial to choose the cutoff mass $\Lambda_K$ for kaon charge from factor and the cutoff mass $\Lambda_N$ for the nucleon charge form factor to describe $d\sigma_L$ and $d\sigma_T$ of $K$ electroproduction, respectively. Inconsistency of $d\sigma_T$ with the VGL and VRN models which favor using the on-shell cutoff mass $\Lambda_N = 0.843$ GeV implies a need for more of the off-shell contributions. We advocate choosing rather a large cutoff mass $\Lambda_N = 1.55$ GeV as demonstrated in the electroproduction of vector meson $\omega$ and $\pi$ for this purpose, avoiding a complication either from the inclusion of $N^*$ resonances or from such a parametrization of nucleon form factor $F_1(Q^2, s)$ as elaborated in Refs. [4, 5].

On the experimental side, there were activities to precisely measure the longitudinal cross section enough to study the internal structure of the meson form factor. R. M. Mohring et al. [10] reported measurements of cross sections for the reaction $^1H(e, e'K^+)Y$, for both the $\Lambda$ and $\Sigma^0$ hyperon states, at an invariant mass of $W = 1.84$ GeV and four-momentum transfers between $0.5 < Q^2 < 2$ (GeV/c)$^2$. $Q^2$ dependence of cross sections $\sigma_{L(T)}$ and their ratio were measured at fixed energy $W = 1.84$ GeV and angle $\theta_K = 0^\circ$ of the produced kaon, where

$$t_{min} = -Q^2 + m_K^2 - 2k_0E_K + 2|\vec{k}||\vec{q}| \qquad (35)$$

in the c.m. frame.

M. Coman et al. [11] studied $^1H(e, e'K^+)\Lambda$ electroproduction in experiment and obtained the dependence of the cross sections $\sigma_{L(T)}/d\Omega$ and $\sigma_U/d\Omega$ upon invariant energy $W$ at $Q^2 = 1.9$ and 2.35 GeV$^2$ with $-t$ fixed at several values.

$$d\sigma_U = d\sigma_T + \epsilon\, d\sigma_L\,. \qquad (36)$$

Solid curves in Fig. 4 shows the cross sections $d\sigma_{L(T)}$ and $d\sigma_U$ compared with the predictions by the Reggeized meson exchanges within the current framework. Since the cross sections were in the energy range $1.8 \leq W \leq 2.14$ GeV, baryon and hyperon resonances are expected to play role in the $s$- and $u$-channels, the separated cross sections reveal a significant disagreement between data and model prediction around $W \approx 2$ GeV not satisfactorily described by existing electroproduction models based on the meson exchange. Such a deviation of the model prediction from experimental data recalls a prominent resonance peak around that energy region. It should be noted that the dotted cross sections predicted by the VRN model describes the resonance peak in the cross section to a degree. The model includes the resonance effect in the nucleon charge form factor as discussed in Eq. (27) together with the modified kaon Regge pole by the slope $\alpha_K$ in Eq. (29).

Influence of the kaon pole on the cross sections was investigated by adopting an off-shell form factor in the Regge model, which better describes the observed energy dependence of $\sigma_T$ and $\sigma_L$.

Recently, M. Carmignotto et al. [12] studied $^1H(e, e'K^+)\Lambda$ electroproduction as a function of the Mandelstam variable $t$ using data from the E01-004 (FPI-2) and E93-018 experiments that were carried out in Hall

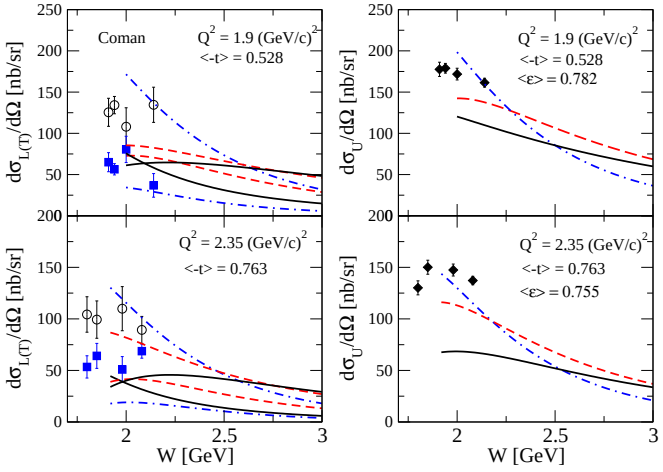


FIG. 5. Energy dependence of $d\sigma_{L(T)}/d\Omega$ and $d\sigma_U/d\Omega$ for $K^+\Lambda$ electroproduction. Momentum-transfer squared $-t$ and electron polarization $\varepsilon$ are taken as average values. Solid curves result from the current model which correspond to $\sigma_T$ (upper curve) and $\sigma_L$ (lower curve) in the left panels, while the dotted are from VRN model with the same notation. Data are taken from Ref. [11].

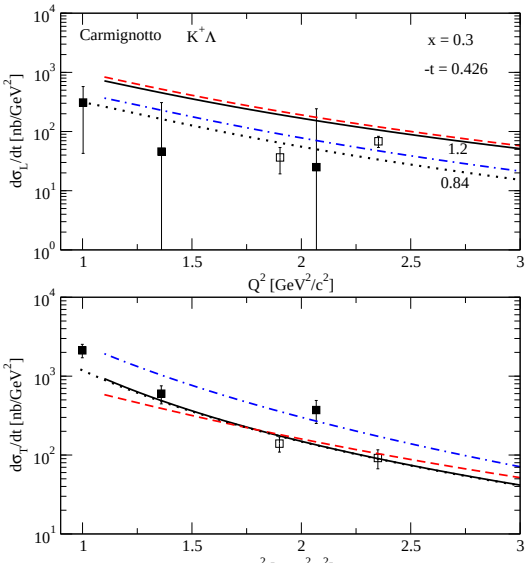


FIG. 6. $Q^2$ dependence of $d\sigma_L$ and $d\sigma_L$ for $K^+\Lambda$ electroproduction. Cross sections from the current model are denoted by solid curves. The (red) dashed curves are predicted by VGL model. The VRN model gives the dotted curves. Data are taken from Ref. [12]

C at the 6 GeV Jefferson Laboratory. The $Q^2$ dependence of the separated cross sections $\sigma_{L(T)}$ at fixed values of $t$ = 0.4 (GeV/c)$^2$ and $x_B$ = 0.3 were presented with the fraction and photon Lab energy defined as,

$$x_B = \frac{Q^2}{W^2 + Q^2 - M_N^2} \ , \tag{37}$$

and

$$\nu = \frac{W^2 - M_N^2 + Q^2}{2M_N} \ . \tag{38}$$

The $Q^2$ dependence of kaon charge form factor were extracted by VGL model [1]. Data from 12 GeV Jefferson Laboratory experiments are expected to have sufficient precision to distinguish between theoretical predictions recent pQCD calculations with modern parton distribution amplitudes. The leading-twist behavior for light mesons is predicted to set in for values of $Q^2$ between 5 and 10 GeV$^2$, which makes data in the few-GeV regime particularly interesting. The $Q^2$ dependence at fixed $x$ and $t$ of the longitudinal cross section that we extracted seems consistent with the QCD factorization prediction within the experimental uncertainty.

### B. Kaon charge form factor

The extraction of the $Q^2$-dependence of kaon form factor $F^K(Q^2)$ from electroproduction is of importance to understand the $q\bar{q}$-substructure of kaon from soft to hard pQCD region [**?** ]. In low $Q^2$ region below around 0.3 GeV$^2$ the kaon form factor is measured from elastic scattering $e + \pi^+ \to e + \pi^+$ [13]. It consistently continues to the form factor in Eq. (21) that is extracted from electroproduction in the intermediate $Q^2$ range with the kaon dominance assumed in the longitudinal component of the hadronic amplitude,

$$\frac{d\sigma_L}{dt} \propto g^2_{\pi NN}(t) F^2_\pi(Q^2, t) \frac{-tQ^2}{(t - m^2_\pi)} \ . \tag{39}$$

The cutoff $\Lambda_K$ of the monopole form factor determines the size of the kaon charge distribution,

$$r_K = \sqrt{6}/\Lambda_K. \tag{40}$$

Such a trend is illustrated in Fig. 8, where the pQCD further predicts the asymptotic saturation in the large $Q^2$ realm,

$$Q^2 F^\pi(Q^2) \to 16\pi\alpha_s f^2_\pi \tag{41}$$

with pion decay constant $f_\pi = 93.1$ MeV.

Therefore, the study of the form factor over large $Q^2$ is indispensable to test pQCD predictions.

### Appendix A: meson-baryon coupling constants from SU(3) symmetry

Table II summarizes the meson-baryon coupling constant of the exchanged meson within the Regge framework for the high-energy photoproduction data. Coupling constants from the Nijmegen soft core potential (NSC$_{97a;f}$) are listed for comparison.

For the consistency-check of the ratio $\alpha = F/D$ in Table II we use the SU(3) relation between the $a_2NN$

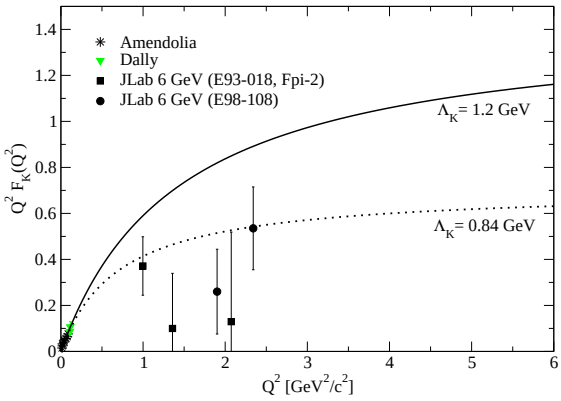


FIG. 7. $Q^2$ dependence of kaon charge form factor. Data are taken from Ref. [12]

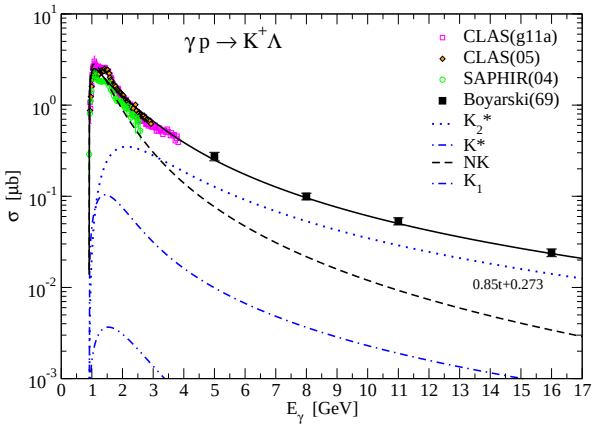


FIG. 8. Total cross section for $K^+\Lambda$ photoproduction up to $E_\gamma = 16$ GeV.

TABLE II. Meson-baryon coupling constants for the exchanged mesons in photoproductions $\gamma N \to \pi^\pm N$ [7] and $\gamma p \to KY$ reactions [6]. The primary coupling constants $g_{Kp\Lambda}$ and $g_{Kp\Sigma}$ are varied within a 20% symmetry breaking. The maximum value is taken for $\gamma K K_2^{*0}$ with negative sign$^{(c)}$.

| | NSC97a | KM [5] | BTK [6] | $\alpha$ |
|---|---|---|---|---|
| $g_{\pi NN}$ | 13.15 | 13.4 | 13.4 | 0.4 |
| $g^v_{\rho NN}$ | 2.97 | 3.4 | 2.6 | 1 |
| $g^t_{\rho NN}$ | 12.52 | 20.74 | 9.62(16.12) | 0.4 |
| $g^v_{a_1 NN}$ | | $7.1 \pm 1.0$ | 6.7 | 0.365 |
| $g^t_{b_1 NN}$ | | - | $-14$ | 0.45 |
| $g^{(1)}_{a_2 NN}$ | | | 1.4 | 2.25 |
| $g^{(2)}_{a_2 NN}$ | | | 0 | 0.21 |
| | NSC97a | VRN/VGL | Present work | |
| $g_{Kp\Lambda}$ | $-13.24$ | $-11.27/-11.54$ | $-11.54$ | |
| $g_{Kp\Sigma^0}$ | 4.11 | 4.6/4.47 | 4.47 | |
| $g_{\gamma K^\pm K^*}$ | | | 0.254 | |
| $g_{\gamma K^0 K^*}$ | | | $-0.388$ | |
| $g^v_{K^* p\Lambda}$ | $-4.26$ | $-1/-23$ | $-4.5$ | |
| $g^t_{K^* p\Lambda}$ | $-11.31$ | $-15.38/-57.5$ | $-16.7$ | |
| $g^v_{K^* p\Sigma^0}$ | $-2.46$ | | $-2.6$ | |
| $g^t_{K^* p\Sigma^0}$ | 1.15 | | 1.924 | |
| $g_{\gamma K^\pm K_1}$ | | | 0.071 | |
| $g_{\gamma K^0 K_1}$ | | | $-0.133^{(a)}$ | |
| $g^v_{K_1 p\Lambda}$ | | $-5.31$ | $-6.7$ | |
| $g^t_{K_1 p\Lambda}$ | | $-7.08$ | 15.36 | |
| $g^v_{K_1 p\Sigma^0}$ | | | 1.81 | |
| $g^t_{K_1 p\Sigma^0}$ | | | $-1.4$ | |
| $g_{\gamma K^\pm K_2^*}$ | | | $0.276^{(b)}$ | |
| $g_{\gamma K^0 K_2^*}$ | | | $< 0.041^{(c)}$ | |
| $g^{(1)}_{K_2^* p\Lambda}$ | | | $-4.45$ | |
| $g^{(2)}_{K_2^* p\Lambda}$ | | | 0 | |
| $g^{(1)}_{K_2^* p\Sigma^0}$ | | | $-4.9$ | |
| $g^{(2)}_{K_2^* p\Sigma^0}$ | | | 0 | |

and the $f_2 NN$ couplings,

$$g^{(1,2)}_{f_2 NN} = \frac{1}{\sqrt{3}}(4\alpha_{(1,2)} - 1)\, g^{(1,2)}_{a_2 NN}, \tag{A1}$$

for $g^{(1(2))}_{f_2 NN} = 6.45(0)$ and $g^{(1(2))}_{a_2 NN} = 1.4(0)$.

Meson- baryon coupling constants for the strangeness sector are determined from the SU(3) relations in Eqs. (A2) and (A3) below [14]. They are consistent with those obtained from the NSC$_{97a}$ [15]. The value $g^{(1)}_{a_2 NN} = 1.4$ or 1.6 is supported by the analyses of the NSC YN potential [15, 16] and its extended version which yield the value $g^{(1)}_{a_2 NN} = 1.57$ [17].

$$g_{KN\Lambda} = -\frac{1}{\sqrt{3}}\,(1 + 2\alpha)\; g_{\pi NN}, \tag{A2}$$

$$g_{KN\Sigma} = (1 - 2\alpha)\; g_{\pi NN}, \tag{A3}$$

### Appendix B: $K^+\Lambda$ photoproduction

Given the meson-baryon coupling constants in the Table II, the total cross section up to photon energy $E_\gamma = 16$ GeV and single spin polarizations, $\Sigma$ and $P$ at $E_\gamma = 16$ and 5 GeV are presented for $\gamma p \to K^+\Lambda$ in Figs. 8 and 9. These are the demonstration of kaon photoproduction with the coupling constants adopted in this work to ensure the validity of its extension to electroproduction. The parameters in the that case are mainly the cutoff $\Lambda_K$ for kaon charge form factor and $\Lambda_N$ for the nucleon charge form factor both of which play the crucial role to determine the longitudinal and transverse cross sections, respectively.

It is interesting to notice that the total cross section cannot agree with high energy data without tensor meson $K_2^*$ exchange. The role of the $K_2^*$ is prominent to reduce the vector meson $K^*$ coupling constants to a large degree. Nevertheless, in the electroproduction, the role of the $K_2^*$ is limited to the transverse component of the cross

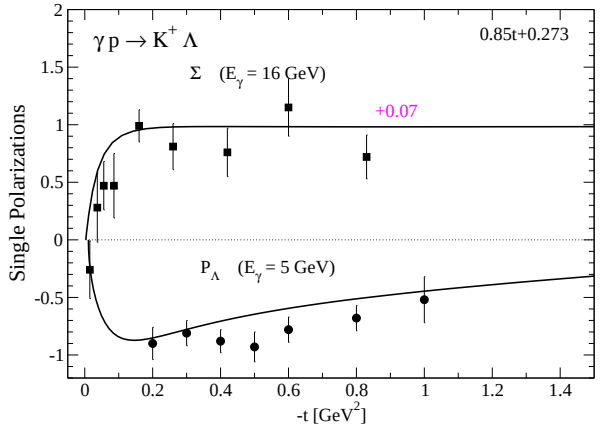


FIG. 9. Beam polarization Σ at $E_\gamma = 16$ GeV and recoil polarization asymmetry at 5 GeV for $K^+\Lambda$ photoproduction.

section $d\sigma_T$. Its role in the electroproduction is likely to be confirmed in the spin polarization. The longitudinal cross section $d\sigma_L$ shows the sensitivity to a change of the kaon exchange.


[1] M. Vanderhaeghen, M. Guidal, and J.-M. Laget, Phys. Rev. C 57, 1454 (1998).
[2] M. Guidal, J.-M. Laget, and M. Vanderhaeghen, Phys. Rev, C 61, 025204 (2000).
[3] F. Gross and D. O. Riska, Phys. Rev. C36, 1928 (1987)
[4] T. Vrancx, J. Ryckebusch, and J. Nys, Phys. Rev. C 89, 065202 (2014); T. Vrancx and J. Ryckebusch, Phy. Rev. C 89, 025203 (2014).
[5] M. M. Kaskulov and U. Mosel, Phys. Rev. C 81, 045202 (2010).
[6] B. G. Yu, T. K. Choi, W. Kim, Phys. Lett. B **701**, 332 (2011).
[7] B.G. Yu, T.K. Choi, W. Kim, Phys. Rev. C 83, 025208 (2011).
[8] B.-G. Yu. Y. Oh, and K.-J.Kong, Phys. Rev. D 95, 074034 (2017).
[9] T. K. Choi, K. J. Kong and B. G. Yu, J. Kor. Phys. Soc. 67, L1089 (2015).
[10] R. M. Mohring *et al.*, Phys. Rev. C 67, 055205 (2003).
[11] M. Coman *et al.*, Phys. Rev. C 81, 052201(R) (2010).
[12] M. Carmignotto *et al.*, Phys. Rev. C 97, 025204 (2018).
[13] Amendolia *et al.*, Nucl. Phys. B 277, 168 (1986).
[14] R. L. Workman and Harold W. Fearing, Phys. Rev. D **37**, 3117 (1988).
[15] Th. A. Rijken, V. G. J. Stoks, and Y. Yamamoto, Phys. Rev. C **59**, 21 (1999); V. G. J. Stoks and Th. A. Rijken, Phys. Rev. C **59**, 3009 (1999).
[16] M. M. Nagels, Th. A. Rijken, and J. J. de Swart, Phys. Rev. D **17**, 768 (1978).
[17] V. G. J. Stoks and Th. A. Rijken, Phys. Rev. C **59**, 3009 (1999).


## Appendix C: Running gfortran code

- The execution file ekaon-btk.out will run by putting " ./ekaon-btk.out " under the gfortran code.
- Choose the reaction $K^+\Lambda$ (1) or $K^+\Sigma^0$ (2)
- Current conservation is checked out and jump over to the next step.
- Model: BTK(1), VGL(2), VRN(3) or BTK with free cut(4)

→ You can select the model, BTK is our model and the cutoff masses in the models of options (1), (2), and (3) are fixed as listed in Table I. Choose (4) if you want to vary the cutoff mass in the BTK model

- WE WILL CALCULATE DIFF. CROSS SECTION(DCS)!!!' WHICH ONE PRINT TO OUT: 4-kinds of DCS & L/T ratio(1), $dS_U$(2), SUM OF 4-DCS(3) OR SSA(4) '

(1)=$d\sigma_T$, $d\sigma_L$, $d\sigma_{TT}$, $d\sigma_{LT}$, and $d\sigma_L/d\sigma_T$

(2)=$d\sigma_U$

(3)=sum of 4 dcs in option (1)

(4) is not relevant to the present calculation

- WE WILL CALCULATE DIFF. CROSS SECTION!!! CHOOSE X-AXIS & FIX VARs. : W,QQ&t(1), QQ,W&t(2), QQ,xb&t(3), QQ,xb&theta(4), QQ,W&theta(5) OR -t,W&QQ(9)

→ (1)=$x$-axis is $W$, $Q^2$ and $t$ are fixed. (2)=$x$-axis is $Q^2$, $W$ and $t$ are fixed. (3)=$x$-axis is $Q^2$, $x_b$ and $t$ are fixed. and so on.

→ if you select (2), you are asked to put the $Q^2$ value for the endpoint of x-axis you want. and then put the $W$ and $t$ as inputs.

→ INPUT: PHOTON POL EL(0¡EL¡1)?; need for $d\sigma_U$ only. If not, PUT ANY VALUE.

- End